

Reduced Naphthylphthalamic Acid Binding in the *tir3* Mutant of Arabidopsis Is Associated with a Reduction in Polar Auxin Transport and Diverse Morphological Defects

Max Ruegger,^{a,1} Elizabeth Dewey,^a Lawrence Hobbie,^{a,2} Dana Brown,^b Paul Bernasconi,^c Jocelyn Turner,^a Gloria Muday,^b and Mark Estelle^{a,3}

^aDepartment of Biology, Indiana University, Bloomington, Indiana 47405

^bDepartment of Biology, Wake Forest University, Winston-Salem, North Carolina 27109

^cNovartis Crop Protection, Research Division, Palo Alto, California 94304

Polar auxin transport plays a key role in the regulation of plant growth and development. To identify genes involved in this process, we have developed a genetic procedure to screen for mutants of Arabidopsis that are altered in their response to auxin transport inhibitors. We recovered a total of 16 independent mutants that defined seven genes, called *TRANSPORT INHIBITOR RESPONSE (TIR)* genes. Recessive mutations in one of these genes, *TIR3*, result in altered responses to transport inhibitors, a reduction in polar auxin transport, and a variety of morphological defects that can be ascribed to changes in indole-3-acetic acid distribution. Most dramatically, *tir3* seedlings are strongly deficient in lateral root production, a process that is known to depend on polar auxin transport from the shoot into the root. In addition, *tir3* plants display a reduction in apical dominance as well as decreased elongation of siliques, pedicels, roots, and the inflorescence. Biochemical studies indicate that *tir3* plants have a reduced number of *N*-1-naphthylphthalamic (NPA) binding sites, suggesting that the *TIR3* gene is required for expression, localization, or stabilization of the NPA binding protein (NBP). Alternatively, the *TIR3* gene may encode the NBP. Because the *tir3* mutants have a substantial defect in NPA binding, their phenotype provides genetic evidence for a role for the NBP in plant growth and development.

INTRODUCTION

Plants have the capacity to modify their growth and development in response to a wide variety of environmental cues. This regulation is accomplished in large part through the action of plant hormones such as indole-3-acetic acid (IAA) or auxin. The primary sites of IAA biosynthesis are thought to be in meristems and young developing organs. IAA is transported to other sites in the plant via a specialized IAA polar transport system. Polar auxin transport has been demonstrated in a wide variety of plant species (Lomax et al., 1995).

Physiological studies suggest that the auxin transport system plays an important role in the regulation of diverse developmental processes, including embryogenesis, stem elongation, apical dominance, leaf abscission, lateral root initiation, and tropisms (Lomax et al., 1995). Many of these studies involve the use of specific inhibitors of polar auxin transport such as *N*-1-naphthylphthalamic acid (NPA) and

related compounds (collectively called phytochemicals). For example, in the case of apical dominance, IAA produced in the apex of the shoot is thought to inhibit the growth of axillary meristems. In classic experiments, the application of NPA just below the apex of a variety of different plant species resulted in the release of dormant axillary buds (Tamas, 1995). These results suggest that IAA is transported to dormant meristems via the polar transport system.

In roots, there is evidence for two streams of auxin transport. In one stream, IAA moves from the shoot into the stele of the root and down toward the root tip (Tsurumi and Ohwaki, 1978; Kerk and Feldman, 1995). In the second stream, IAA moves through epidermal cell files in a basipetal direction away from the root tip (Meuwly and Pilet, 1991). These two transport streams appear to have particular importance for different developmental processes. Auxin synthesized in the shoot and transported into the root is required for lateral root development. Removal of the auxin-synthesizing tissues (e.g., the cotyledons) (Wightman and Thimann, 1980) or treatment of seedlings with NPA abolishes lateral root formation (Muday and Haworth, 1994; Reed and Muday, 1996). It is not clear what role, if any, IAA from the shoot plays in primary root elongation. However, experiments with maize

¹ Current address: Department of Biochemistry, Purdue University, West Lafayette, IN 47907.

² Current address: Department of Biology, Adelphi University, Garden City, NY 11530.

³ To whom correspondence should be addressed. E-mail mestelle@bio.indiana.edu; fax 812-855-6705.

have shown that IAA applied to the base of the root accumulates in the root tip, suggesting that shoot-derived IAA has a role in root elongation (Kerk and Feldman, 1995). The epidermal transport stream may play a key role in gravitropism (Evans, 1991; Meuwly and Pilet, 1991). Treatment of seedlings with low concentrations of NPA abolishes gravitropism, indicating that this process depends on regulated auxin transport (Muday and Haworth, 1994; Reed and Muday, 1996).

According to our current understanding, polar auxin transport requires the action of cellular IAA influx and efflux carriers (Lomax et al., 1995). A specific influx carrier has been proposed because IAA uptake into stem segments, protoplasts, or purified membrane vesicles is partly saturable by IAA or the synthetic auxin 2,4-D (Davies and Rubery, 1978). Recently, Bennett et al. (1996) demonstrated that the *AUX1* gene of *Arabidopsis* encodes a protein related to amino acid permeases and suggested that this protein may function as an influx carrier.

The auxin efflux carrier was defined using transport inhibitors such as NPA (Katekar and Geissler, 1977). These compounds bind to a single high-affinity binding site, the NPA binding protein (NBP; Muday et al., 1993), and inhibit cellular auxin efflux. The NBP has not been purified, and its function is not known. One possibility is that the NBP acts to regulate auxin efflux. Consistent with this model, experiments with protein synthesis inhibitors suggest that the NBP and the efflux carrier are distinct proteins (Morris et al., 1991). In addition, several studies with zucchini hypocotyls suggest that the NBP is a peripheral membrane protein that is localized to the cytoplasmic face of the membrane and associated with the cytoskeleton (Cox and Muday, 1994; Dixon et al., 1996). However, Bernasconi et al. (1996), also working with zucchini, found that the NPA binding site is highly resistant to digestion by proteinase K and suggested that the protein is integral to the membrane. This result is consistent with a model in which the NBP is part of the efflux carrier. Finally, it is formally possible that the NBP does not normally function in auxin transport but disrupts transport when it is complexed with NPA. Further genetic and biochemical studies are required to establish the function of the NBP.

Five *Arabidopsis* mutants have been identified with defects in auxin transport or NPA response. Three of these, *pin-formed* (*pin*), *pinoid* (*pid*), and *monopteros* (*mp*), also result in the formation of aberrant inflorescences and floral meristems (Okada et al., 1991; Bennett et al., 1995; Przemeczek et al., 1996). The *mp* mutant was originally isolated as a seedling lethal mutant (Berleth and Jurgens, 1993) but was recently shown to be affected in inflorescence morphology, vascular development, and auxin transport. Another mutant with a defect in vascular development, called *lopped* (*lop1*), has reduced auxin transport (Carland and McHale, 1996). The fifth mutant, *roots curl in NPA* (*rcn1*), displays differences in NPA response that appear to be consistent with an increase in NPA sensitivity (Garbers et al., 1996). The *RCN1* gene has been cloned and encodes a phosphatase regula-

tory subunit, suggesting that phosphorylation is involved in regulation of auxin transport. The *rcn1* mutation does not affect NPA binding. NPA binding experiments have not been reported for *pin*, *pid*, or *lop1*.

In an effort to identify additional gene products that are involved in auxin transport, we have screened for *Arabidopsis* mutants that have altered responses to auxin transport inhibitors such as NPA. The *transport inhibitor response* (*tir*) mutants exhibit altered responses to these inhibitors as well as auxin-related growth defects. In this report, we focus on the *tir3* mutants. Our results indicate that the *TIR3* gene is required for synthesis, localization, or function of the NBP. A reduction in the number of NPA binding sites in the *tir3* mutant is associated with reduced auxin transport and a variety of auxin-related growth defects, including a dramatic reduction in the number of lateral roots.

RESULTS

Screening for Mutants Affected in Auxin Transport

Phytotropins, such as NPA, 2-carboxyphenyl-3-phenylpropane-1,2-dione (CPD), or methyl-2-chloro-9-hydroxyfluorene-9-carboxylate (CFM), inhibit polar auxin transport by inhibiting cellular IAA efflux. When *Arabidopsis* seedlings are grown on medium containing phytotropin, the roots display a characteristic response. There are three components to this response. (1) Lateral root formation is inhibited at extremely low concentrations (0.05 μM). (2) At slightly higher concentrations, root gravitropism is disrupted. (3) At ~ 0.1 μM and higher, root elongation is inhibited and the root tip swells (Figures 1 and 2). A similar set of responses is observed in other plant species (Muday and Haworth, 1994; Muday et al., 1995). To define genes whose products are involved in auxin transport, we have used the seedling response to NPA to screen for NPA/CPD/CFM-resistant mutants. A total of 120,000 M_2 seedlings were plated on medium containing 5 μM NPA, 5 μM CPD, or 0.1 μM CFM (see Methods for details). Twenty-six recessive mutants that displayed increased root elongation on these compounds were recovered. Subsequent studies showed that each of the mutants is resistant to NPA, CPD, and CFM. Genetic analyses indicated that 10 of the mutants had mutations in the *AXR1* gene and were also resistant to auxin. The remaining 16 mutants defined seven new *TIR* genes (*TIR1* through *TIR7*).

The number of mutant alleles of each gene recovered is indicated in Table 1. Six of the genes (*TIR2* through *TIR7*) were mapped by crossing a homozygous mutant plant in the Columbia (Col-0) background to a wild-type plant in the Landsberg *erecta* (Ler-0) background. Mutant F_2 plants were recovered, and DNA was isolated from each plant. The segregation of the *Arabidopsis* restriction fragment length polymorphism set (ARMS) and simple sequence length polymorphism markers was determined by DNA gel or polymerase

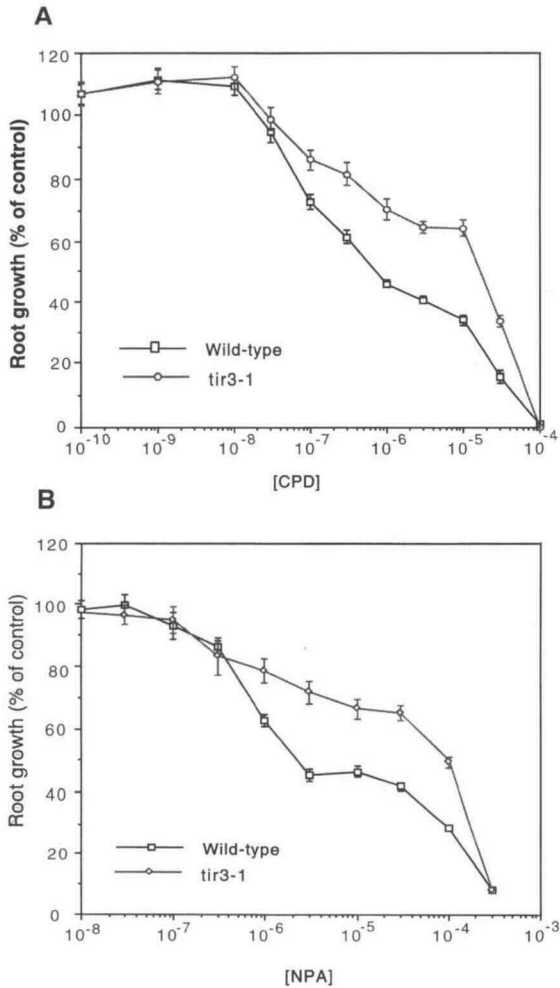


Figure 1. Growth of Wild-Type and *tir3-1* Seedling Roots on NPA and CPD.

Three-day-old wild-type and *tir3-1* seedlings were transferred to medium containing various concentrations of NPA or CPD. Root growth over the next 5 days was recorded and expressed as a percentage of root growth on medium without an inhibitor.

(A) Root growth on CPD.

(B) Root growth on NPA.

Error bars represent the standard error. At least 12 seedlings were measured for each data point. Root length on medium without an inhibitor was 42.2 ± 2.9 mm ($n = 24$) for the wild type and 34.5 ± 3.0 mm ($n = 24$) for *tir3-1*.

chain reaction (PCR), respectively. The results of this analysis are shown in Table 1. This article focuses on the *TIR3* gene. Two mutant alleles of this gene, called *tir3-1* and *tir3-2*, were recovered from diepoxybutane-mutagenized populations. The two alleles have a similar phenotype. The *tir3-1* mutant was designated the reference allele and characterized in detail.

***tir3* Mutants Display Altered Responses to Phytotropins**

The *tir3* mutants were recovered by screening for seedlings with increased root elongation on phytotropin. To fully characterize the response of the *tir3-1* mutant to phytotropin, we determined the effects of NPA or CPD on root elongation and root tip morphology. The effects of these compounds on root elongation are shown in Figures 1A and 1B. Using a 50% inhibitory concentration (IC_{50}) as an indication of sensitivity, we found that *tir3-1* is between 20- and 50-fold less sensitive to phytotropin than is the wild type.

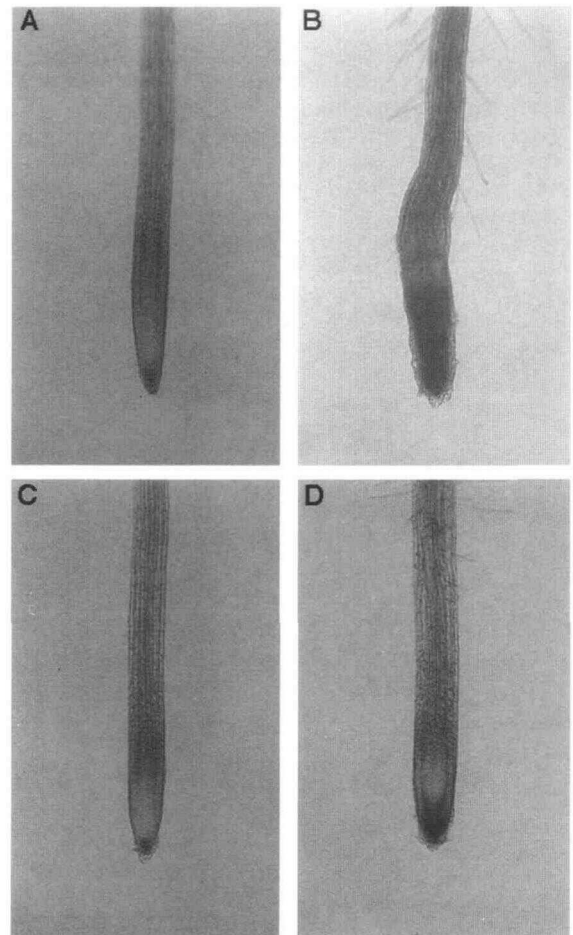


Figure 2. Morphology of Wild-Type and *tir3-1* Roots Exposed to CPD.

Seedlings were grown for 7 days and photographed using a dissecting microscope.

(A) Wild-type seedling grown on minimal medium.

(B) Wild-type seedling grown on minimal medium plus 5 μ M CPD.

(C) *tir3-1* seedling grown on minimal medium.

(D) *tir3-1* seedling grown on minimal medium plus 5 μ M CPD.

Table 1. *TIR* Complementation and Mapping^a

Locus	No. Independent Alleles	Marker	Chromosomes ^b		Map Position ^c
			NR	R	
<i>TIR1</i>	5				
<i>TIR2</i>	4	315B	43	5	1:145
		453A	47	1	
<i>TIR3</i>	2	nga172	46	4	3:0
		560B2	36	12	
<i>TIR4</i>	1	254A	33	13	1:120
		315B	43	3	
<i>TIR5</i>	2	217C	31	11	5:50
		247A	30	13	
<i>TIR6</i>	1	448A	41	5	4:15
		326B	33	13	
<i>TIR7</i>	1	217C	41	1	5:20
		247A	31	15	

^aThe *TIR1* locus was mapped by the method of Lister and Dean (1993; recombinant inbred lines). The remaining loci were mapped with respect to the indicated marker loci by using the methods of Fabri and Schäffner (1994; ARMS) or Bell and Ecker (1994; simple sequence length polymorphism markers).

^bThe number of nonrecombinant (NR) or recombinant (R) chromosomes scored at the marker position shown.

^cChromosome and approximate map position with respect to the Arabidopsis recombinant inbred map (NASC <http://nasc.nott.ac.uk/>). Linkage distances were derived using the Haldane mapping function (see Koornneef and Stam, 1992).

In addition to inhibiting root elongation, phytohormones have a profound effect on morphology of the root tip. After several days on the inhibitor, the tips of wild-type seedlings became significantly swollen (Figures 2A and 2B). This swelling was less pronounced in *tir3* seedlings (Figures 2C and 2D). To determine the cause of root tip swelling, sections from treated and untreated wild-type and *tir3* roots were examined. The results are shown in Figure 3. The Arabidopsis root has a relatively invariant cellular organization maintained in the postembryonic root by a series of stereotypical cell divisions in the meristematic initials and their derivatives (Figures 3A and 3E). The meristem has a closed organization with three tiers of initials lying above the root cap (Dolan et al., 1993). Treatment of wild-type seedlings with CPD caused dramatic changes in this organization (Figure 3C, 3G, and 3I). The initials were no longer arranged in three tiers, and the meristem had a more open appearance without a clear demarcation between the initials and the root cap. Unprogrammed periclinal cell division resulted in a large increase in the number of cell files in CPD-treated wild-type roots, particularly distal from the root tip. This is most clearly evident in Figures 3E, 3G, and 3I. It was no longer possible to clearly identify cortical and epidermal cell layers in these roots. In addition, the zone of cell division, characterized by

isodiametric cell shape, was greatly expanded in CPD-treated roots. In untreated roots, the cell division zone comprised the distal 250 μm (data not shown), whereas in treated roots, this zone extended back ~ 500 μm from the root tip (Figure 3I). As a consequence, the zone of cell elongation was displaced distally. These changes suggest that auxin and perhaps gradients of auxin concentration are important for organization of the meristem.

When grown on minimal medium, *tir3-1* roots are similar to the wild type in appearance (Figures 3B and 3F). The columella cell files are straighter in *tir3-1* seedlings than in wild-type seedlings, giving the root cap a more closed appearance. The effects of CPD on *tir3* root structure were much less pronounced than those seen in the wild type. A moderate increase in cell number was observed, and the tissue was much better organized than in wild-type CPD-treated roots (Figures 3D, 3H, and 3J). It was still possible to identify the central cells as well as epidermal and cortical cell files in these sections. Similarly, the elongation zone was only slightly displaced compared with untreated roots (Figure 3I). Based on these results, we conclude that exposure to the auxin transport inhibitor causes aberrant cell division in the root tip, resulting in a disruption of meristem organization, an increase in the size of the division zone, and displacement of the elongation zone. The *tir3-1* mutation acts to reduce these effects.

It is worth noting that the seedlings' response to phytohormone is very different from the seedlings' response to auxin (Muday et al., 1995). Treatment of seedlings with an active auxin has little effect on gravitropism in Arabidopsis and stimulates lateral root development in most plants. Although auxin and phytohormone both inhibit root elongation, the effects of these two compounds on root morphology are quite different. In particular, auxin does not promote the organized swelling that is observed after phytohormone treatment. Instead, cells in the epidermis swell and peel away from the underlying cortical layer. Prolonged exposure results in generation of completely disorganized callus tissue. Presumably, these differences are due to the mode of action of the two compounds. Treatment with phytohormone results in changes in the distribution of endogenous auxin within the organ, whereas auxin treatment causes an increase in auxin levels in all tissues of the root.

The *tir3* Phenotype Is Not Caused by a Defect in Auxin Response

The results described above suggest that the *tir3-1* mutants are impaired in auxin transport and as a consequence display altered responses to phytohormone. However, because phytohormones act to increase intracellular auxin levels by inhibiting efflux, a mutation affecting auxin response would also alter a response to phytohormones. In fact, 10 new *axr1* mutants were recovered in our screen. To determine whether the *tir3* mutants are less sensitive to auxin, we examined the re-

sponse of *tir3-1* seedlings to IAA and the synthetic auxin 2,4-D. In this assay, *tir3* roots were only slightly resistant to auxin compared with the wild type, suggesting that altered response to phytotropin is probably not due to a decrease in auxin responsiveness (data not shown).

The *tir3-1* Mutants Have Reduced IAA Transport in the Inflorescence

Because of the small size of the Arabidopsis seedling, it is difficult to measure IAA transport in either the hypocotyl or root. Instead, we measured polar IAA transport in inflorescence segments, as described by Okada et al. (1991). Figure 4 shows that in the wild type, auxin begins to accumulate in the basal part of the segment within 2 hr and continues to accumulate throughout the experiment. This transport is inhibited by NPA. Polar auxin transport was also detectable within 2 hr in *tir3-1* segments, indicating that the initial velocity of transport was similar for the two genotypes. However, the amount of IAA transported in *tir3-1* stems was significantly reduced when compared with that in the wild type. At 18 hr, the total IAA transported in *tir3-1* stems was ~30% of that found in wild-type stems. Acropetal transport was also measured in both genotypes and found to be much lower than basipetal transport, but it was similar in both wild-type and *tir3-1* tissues (data not shown).

To determine whether reduced IAA transport in *tir3-1* stems is associated with gross changes in stem morphology, we examined sections of wild-type and *tir3-1* stems with the scanning electron microscope. Figures 5A and 5B show that *tir3-1* stem tissue has an organization similar to that of wild-type stems. The thickness of Arabidopsis stems for both the wild type and *tir3-1* is somewhat variable, and as shown in Figure 5, the *tir3-1* stem is thicker and has more vascular bundles. However, in other respects, the *tir3-1* stem is similar to wild-type stems in appearance. Figures 5C and 5D show a vascular bundle from wild-type and *tir3-1* stems. All of the cell types present in the wild-type stem are also present in *tir3-1* stem. In particular, the cortical cells directly adjacent to the phloem are similar in size and number in wild-type and *tir3-1* stems. These cells are thought to be the major site of polar auxin transport in dicot stems (Morris and Thomas, 1978).

Decreased IAA Transport Is Associated with Reduced Numbers of NPA Binding Sites in Microsomes

To determine whether resistance to NPA and CPD is associated with changes in NPA binding, we analyzed NPA binding in microsomes prepared from 3-day-old etiolated seedlings. High background binding in these preparations (46% of total counts) precluded a saturation analysis. However, at 10 nM NPA concentrations, microsomes from *tir3* seedlings consistently displayed lower ³H-NPA binding activity

than did microsomes from wild-type seedlings (Figure 6). In a typical experiment, *tir3-1* microsomes had 41% (0.2 pmol/mg protein) of the NPA binding activity of wild-type microsomes (0.5 pmol/mg protein).

NPA binding studies using microsomes prepared from mature rosettes indicated that this material had less background binding than did microsomes from seedlings. A saturation curve of ³H-NPA binding over a range of concentrations is shown in Figure 7. The background at the highest concentration is <25% of the total. In the presence of detergent, ³H-NPA binding was sensitive to digestion by protease, indicating that this assay measures the binding of NPA to a protein site. From similar saturation data, Lineweaver-Burk plots of NPA binding were constructed for wild-type and *tir3-1* microsomes. The Lineweaver-Burk plots were used to calculate the dissociation constant (K_d), which describes the affinity of the protein for NPA, and the B_{max} , which estimates the number of NPA binding sites in the preparation. Values that are the average of three separate experiments are reported in Table 2. The affinity of the NBP for NPA in these two genotypes was similar, but there is a threefold lower abundance of NPA binding activity in the *tir3* microsomes prepared from rosettes compared with those of the wild type. Student's *t* tests were performed to analyze the difference between the wild-type and *tir3-1* values. For B_{max} , a $P < 0.05$ indicates that the values are statistically different. In contrast, the K_d values exhibited no statistical difference with a $P > 0.2$. A similar study was performed with microsomes prepared from mature root tissue. In this case, background binding was considerably higher than in rosette tissue. Nonetheless, the B_{max} in *tir3-1* microsomes was also twofold lower than that observed in microsomes from wild-type roots ($P < 0.001$), whereas the K_d values were similar ($P > 0.2$; Table 2). These results indicate that the number of NPA binding sites is reduced in seedlings as well as in roots and rosettes of mature *tir3-1* plants.

The *tir3* Mutants Are Deficient in Organ Elongation and Lateral Root Development

The *tir3* mutants have a distinctive phenotype that is characterized by a reduction in the length of all elongating organs and the near absence of lateral roots in seedlings. Figures 8A to 8D illustrate the rosette and inflorescence morphology of *tir3-1* and wild-type plants. Morphometric analyses of these plants are summarized in Table 3. These data show that elongation of all organs was reduced in *tir3-1* plants, including inflorescences, siliques, pedicels, and roots. Measurement of epidermal cell length indicated that cell length was similar to that of the wild type in the root but reduced in the inflorescence. Thus, the decrease in organ elongation appears to be due to changes in both cell division and/or cell elongation, depending on the organ. In addition to the elongation defect, *tir3-1* plants had decreased apical dominance.

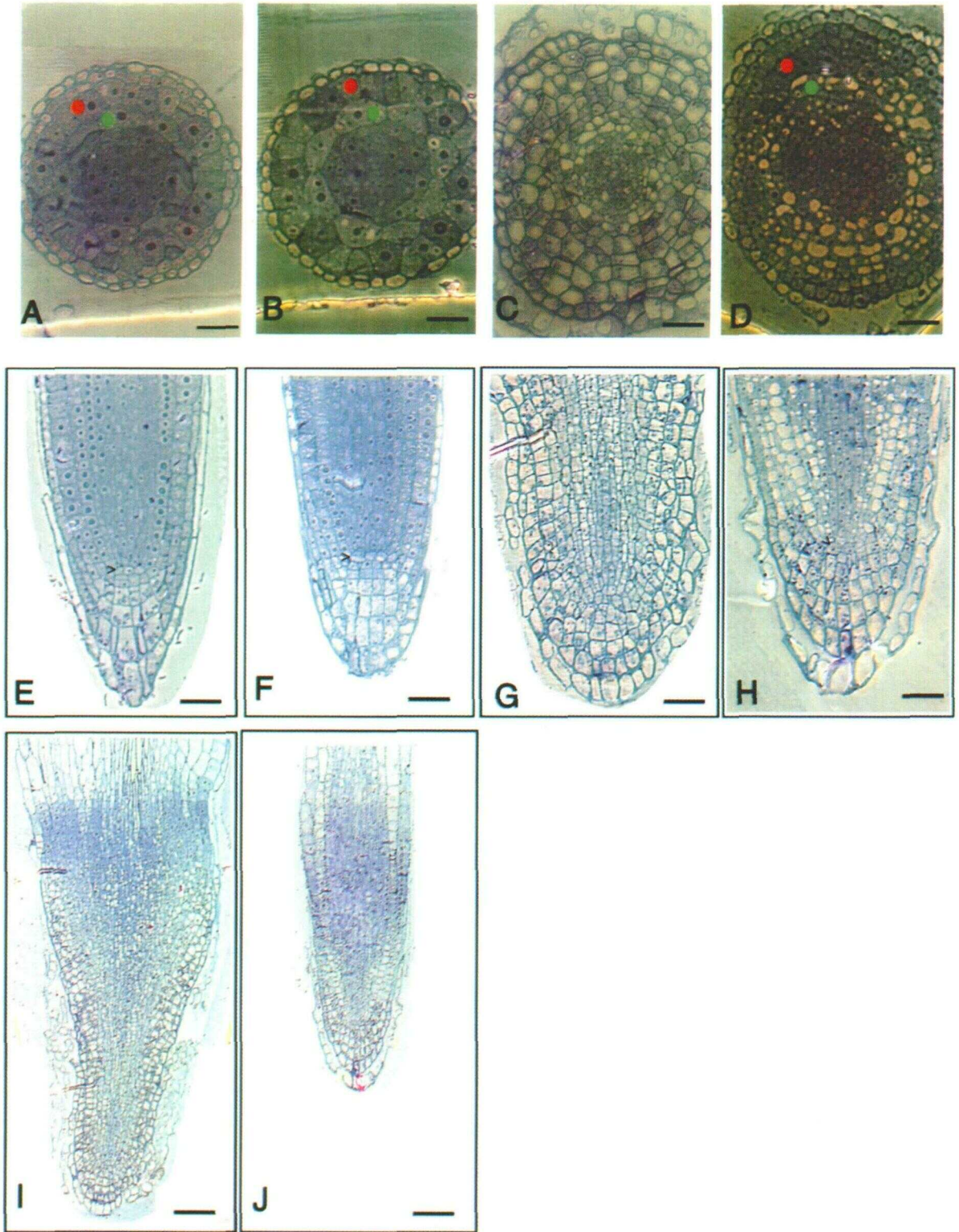


Figure 3. Effect of CPD on Cellular Organization of Wild-Type and *tir3-1* Roots.

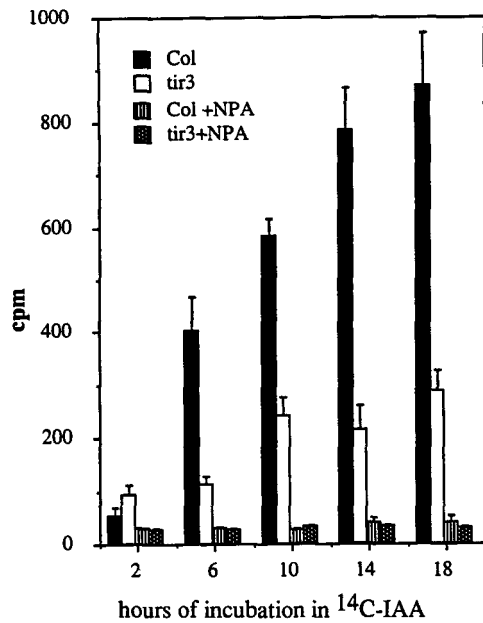


Figure 4. Polar Auxin Transport in Wild-Type and *tir3-1* Inflorescence Stems.

Two and one-half centimeters of stem was excised, and the apical end was placed in a nutrient solution containing 1 μM ^{14}C -IAA for the times indicated. The amount of radioactive IAA transported to the basal end of the stem was assayed by liquid scintillation. Each column represents the mean of three replicates, and the bar represents the standard error of the mean.

Mutant plants had more than twice the number of secondary inflorescences compared with the wild type.

One of the most striking defects in *tir3* seedlings was a dramatic reduction in lateral root formation (Figures 8E and 8F). When grown on agar medium for 10 days, most *tir3-1* seedlings had no lateral roots, whereas wild-type seedlings had an average of 6.3 ± 0.4 ($n = 10$) lateral roots. When mutants were grown on medium supplemented with IAA or 2,4-D, they developed lateral roots of normal appearance, indicating

that the *tir3-1* defect does not reflect a general inability to form a lateral root meristem (data not shown).

DISCUSSION

A Screen for Mutants Affected in Auxin Transport and Auxin Response

Auxin transport inhibitors such as NPA inhibit root elongation in *Arabidopsis* seedlings. Previous studies with tomato suggest that the effect of NPA on elongation growth is due to the accumulation of IAA in the root tip (Muday and Haworth, 1994; Muday et al., 1995). We have used the NPA response to screen for new *Arabidopsis* mutants that are affected in auxin transport and/or auxin response. Seven new genes (*TIR1* through *TIR7*) were identified in this screen. To date, we have characterized the *tir1* and *tir3* mutants in detail. The *tir1* mutants, like the *axr1* mutants, are resistant to auxin as well as NPA and are affected in auxin response (M. Ruegger, E. Dewey, W. Gray, L. Hobbie, J. Turner, and M. Estelle, unpublished data). In contrast, the results described here suggest that the *TIR3* gene functions in auxin transport.

Decreased Levels of the NBP Are Associated with Reduced IAA Transport

The effects of NPA on auxin efflux and polar auxin transport suggest that the NBP has an important role in these processes. Further, Suttle (1991) demonstrated a correlation between the level of NPA binding activity and the amount of IAA transported in sunflower stem segments, suggesting that the NBP has a positive role in IAA efflux. Our results with the *tir3-1* mutant provide strong support for this view. NPA binding studies indicate that microsomes prepared from *tir3-1* rosettes, roots, and seedlings have 50 to 70% fewer NPA binding sites than do microsomes from wild-type tissues, whereas the K_d value for binding was similar for both genotypes. These differences are associated with a large reduction in the amount of IAA transported in the stem. The relationship between the *TIR3* gene and the NBP is uncertain.

Figure 3. (continued).

(A) to (D) Cross-sections of roots 300 μm from the root tip. (A) and (C) are from wild-type seedlings grown on minimal medium and minimal medium plus 5 μM CPD, respectively. (B) and (D) are from *tir3-1* seedlings grown on minimal medium and minimal medium plus 5 μM CPD, respectively.

(E) to (J) Medial longitudinal sections of root tips from seedlings. (E), (G), and (I) are from wild-type seedlings grown on minimal medium (E) or minimal medium plus 5 μM CPD [(G) and (I)]. (F), (H), and (J) are from *tir3-1* seedlings grown on minimal medium (F) or minimal medium plus 5 μM [(H) and (J)].

In (A), (B), and (D), the red dots indicate the epidermal cell layer, and the green dots indicate the cortical cell layer. Bars in (A) to (H) = 20 μm ; bars in (I) and (J) = 50 μm .

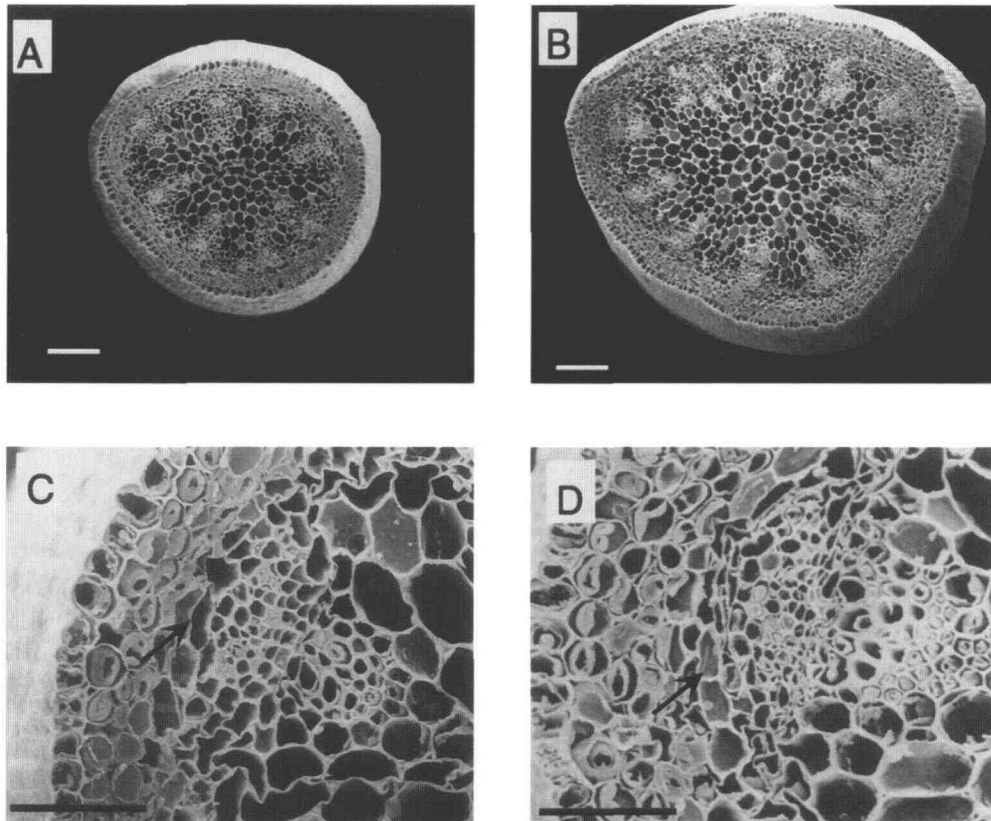


Figure 5. Scanning Electron Microscopy of Sections Prepared from Wild-Type and *tir3-1* Stems.

(A) and **(B)** Cross-sections of wild-type and *tir3-1* stems, respectively. Sections are from stem segments collected in the apical 2 cm of inflorescences after 44 days of growth.

(C) and **(D)** Higher magnification of sections viewed in **(A)** and **(B)**, respectively.

Arrows in **(C)** and **(D)** indicate cortical cells implicated in polar auxin transport. Bars in **(A)** and **(B)** = 100 μm ; bars in **(C)** and **(D)** = 40 μm .

It is possible that the *TIR3* gene encodes the NBP and that the *tir3* mutations result in reduced protein levels. Alternatively, *TIR3* could be involved in synthesis and/or localization of the NBP. A third possibility is that the gene encodes a protein that interacts with the NBP, and in its absence, the NBP becomes destabilized. We expect that the molecular characterization of *TIR3* will help determine which of these possibilities is correct.

Role of *TIR3* and Auxin Transport in Plant Development

The *tir3* mutants display a variety of growth defects. Although other possibilities cannot be excluded, the simplest explanation for these defects is altered IAA distribution resulting from a defect in polar auxin transport. Several aspects of the *tir3* root phenotype are consistent with a reduction in IAA transport into the root system. First, root

growth in *tir3* seedlings is resistant to the effects of NPA. Muday et al. (1995) have suggested that in tomato, NPA inhibition of root elongation is caused by IAA accumulation in the root tip. Our results, including the behavior of the auxin-resistant mutant *axr1*, indicate that this is true in Arabidopsis as well. If *tir3* seedlings have the same transport defect that we have demonstrated in mutant stem segments, then less IAA is transported into the seedling root. Consequently, when mutant seedlings are treated with NPA, lower levels of IAA accumulate in the root tip compared with those in the wild type, and growth inhibition is less severe. Although we have not measured IAA transport in seedlings, the reduction in NPA binding activity in these tissues makes it likely that transport is reduced in this tissue as it is in stems. Second, *tir3* seedlings have a dramatically reduced number of lateral roots. Studies have shown that lateral root initiation is dependent on IAA transported from the shoot into the root (Wightman and Thiman, 1980; Reed and Muday, 1996).

Thus, in the case of *tir3*, the absence of lateral roots can be explained by decreased auxin transport from the shoot. Consistent with this hypothesis, we found that treatment of *tir3* roots with 2,4-D induces a normal number of lateral roots (E. Dewey and M. Estelle, unpublished data). Because 2,4-D is not a good substrate for the auxin efflux carrier (Delbarre et al., 1996), polar auxin transport presumably does not play a role in lateral root induction with this compound.

Another aspect of the *tir3* phenotype is reduced organ length in the inflorescence, silique, pedicel, and root. Experiments with applied NPA in a variety of plants clearly implicate auxin transport in elongation growth (Lomax et al., 1995). If a growing stem is girdled with NPA, elongation increases above the site of application and decreases below the girdle. Thus, in *tir3* plants, stem elongation may be reduced because less IAA is being transported from the meristem into the elongation zone. Consistent with this model, we found that cell length is reduced in *tir3* stems relative to those of the wild type. The situation is somewhat different for *tir3* roots, in which a reduction in growth is associated with a change in cell number rather than cell length. This may be because cell division in the root tip is dependent in part on auxin that is transported from the shoot system. We suggest that less auxin is moving into the root system in *tir3* plants, thus resulting in reduced cell division in the root tip.

The phenotype of *tir3* plants as well as the effects of NPA on wild-type plants strongly suggest that regulated move-

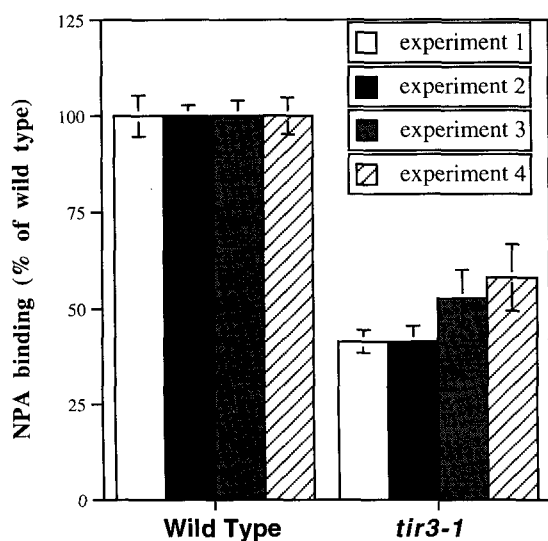


Figure 6. ^3H -NPA Binding to Microsomes Prepared from Etiolated Wild-Type and *tir3-1* Seedlings.

Individual results from four independent experiments are reported. Values are given as a percentage of NPA binding in the wild type. Representative specific binding in the wild type was 0.5 pmol/mg of protein (0.68 total for 0.18 nonspecific). Bars represent standard errors.

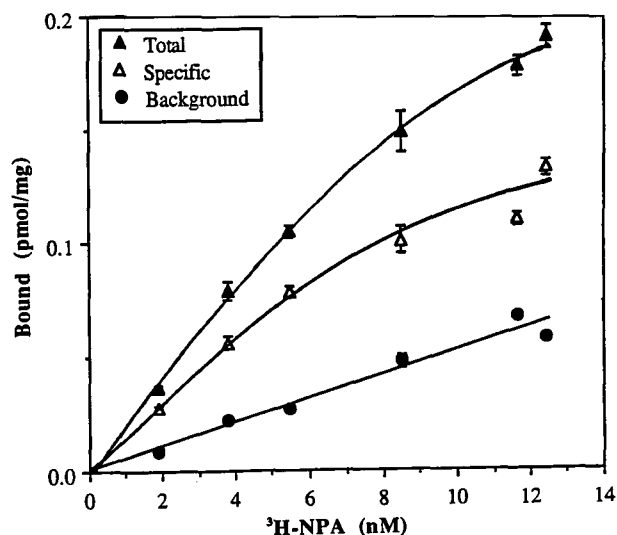


Figure 7. Saturation Curve of ^3H -NPA Binding to Microsomal Membrane Preparation from Wild-Type Rosettes.

Total, specific, and background binding were determined over a range of 2 to 10 nM ^3H -NPA after incubation for 1 hr at 4°C. Background or nonspecific binding was determined by the addition of 10 μM unlabeled NPA to each ^3H -NPA concentration. The average background in this experiment was calculated to represent 23% of total binding. Bars represent standard errors.

ment of IAA plays a key role in plant development. As has been proposed previously, the NBP may function as a regulator of IAA transport. Thus, plants could control IAA level and distribution by regulating the levels of NBP. In addition, it is possible that a natural NBP ligand such as a flavonoid may be involved in regulation of transport (Jacobs and Rubery, 1988). We expect that the molecular characterization of the *TIR3* gene as well as other *TIR* loci will provide important new insights into the mechanism and regulation of auxin transport.

Organization of the Root Meristem Is Disrupted by Changes in IAA Levels

Because auxin is essential for division of plant cells in culture, it is likely to play a key role in meristem function. In the case of lateral root meristems, it is clear from both physiological and genetic studies that auxin is required for initiation and maintenance of the meristem and continued growth of the lateral root (Celenza et al., 1995; Hobbie and Estelle, 1995). The situation in the root apex is less clear. Kerk and Feldman (1994, 1995) proposed that IAA has a special role in maintaining the quiescent center of the root meristem. In their experiments, 2,3,5-triiodobenzoic acid (another auxin transport inhibitor) was applied 2 cm back from the root tip of maize seedlings. The effect of this treatment is to stimulate

Table 2. Comparison of $^3\text{H-NPA}$ Binding Constants^a in Wild-Type and *tir3-1* Microsomes Prepared from Rosette Tissue

Tissue Source	Wild Type (B_{max})	<i>tir3-1</i> (B_{max})	Wild Type (K_d)	<i>tir3-1</i> (K_d)
Rosettes	0.31 ± 0.06	0.11 ± 0.02	17 ± 4.4	24 ± 6.2
Roots	0.03 ± 0.007	0.015 ± 0.004	10 ± 1.8	6.2 ± 1.5

^a Reported values were derived from Lineweaver-Burk plots and represent the average and standard error of three separate experiments with six connections of $^3\text{H-NPA}$. K_d is calculated as $-1/x$ intercept; B_{max} is defined as $1/y$ intercept.

unusual periclinal divisions in the meristem, resulting in the loss of the closed meristem structure typical of maize. The boundary between the root cap and the root proper becomes obscure. We observed similar changes in NPA-treated *Arabidopsis* seedlings. These experiments indicate that changes in IAA concentration can have a profound effect on organization of the meristem. Also, the meristem in *tir3-1* mutants (untreated) is more closed than in wild-type roots, possibly because of decreased IAA levels in the mutant meristem.

In addition to affecting the meristematic initials and the root cap, NPA dramatically expands the size of the cell division zone and displaces the elongation zone back from the root tip in wild-type plants. Cells with an isodiametric shape extend up to 500 μm back from the root tip in treated roots, compared with ~ 250 μm for untreated roots. At 500 μm , there is a very sharp transition between isodiametric cells and elongated cells of relatively normal size. Apparently, cell elongation is not inhibited once the cells are a sufficient distance away from the root tip. These results suggest that the transition from cell division zone to elongation zone may involve changes in IAA concentration. We propose that in an untreated root, there is a concentration gradient of IAA, with highest levels at the root tip and decreasing levels at positions farther back from the tip. At higher IAA concentrations, cell division is favored. As cells move away from the meristem, IAA levels decrease, cell division ceases, and cells elongate to their mature size. In NPA-treated roots, the IAA concentration gradient may be altered such that IAA levels are high enough to promote cell division farther back from the tip. Additional studies are required to confirm this model. In particular, it would be interesting to examine roots that have much lower IAA levels in the root tip.

METHODS

Plant Materials and Growth Conditions

All mutant lines were in the *Arabidopsis thaliana* Columbia (Col-0) ecotype. Plants were grown at 21 to 23°C under continuous fluores-

cent illumination (100 to 150 $\mu\text{E m}^{-2} \text{sec}^{-1}$) in 13-cm clay pots containing Metro-Mix (W.R. Grace and Co., Milpitas, CA) or an equivalent soilless mixture. During the first 3 weeks of growth, a mineral nutrient solution containing 5 mM KNO_3 , 2.5 mM KPO_4 (adjusted to pH 5.5), 2 mM MgSO_4 , 2 mM $\text{Ca}(\text{NO}_3)_2$, 50 μM Fe-EDTA, 70 μM H_3BO_3 , 14 μM MnCl_2 , 0.5 μM CuSO_4 , 1 μM ZnSO_4 , 0.2 μM Na_2MoO_4 , 10 μM NaCl, and 10 nM CoCl_2 was supplied to the plants. For many experiments, plants were grown under sterile conditions in Petri plates containing this nutrient solution plus 0.7% agar, 1% sucrose (w/v), and various hormones or inhibitors as indicated. Before plating, seeds were surface sterilized by agitation for 10 to 20 min in 20% commercial bleach and 0.02% Triton X-100, rinsed several times with sterile water, and held at 4°C for 4 days to enhance germination. The seeds were dispersed on the growth media with sterile water. The plates were oriented vertically and held in an incubator containing fluorescent lighting (30 to 50 $\mu\text{E m}^{-2} \text{sec}^{-1}$ with a 16-hr photoperiod) and at a temperature of 20 to 21°C. In all experiments in which plants were grown, day 0 is considered to be the time when seeds were first placed in the growth conditions described above.

Isolation of Mutants

For chemical mutagenesis, seeds were soaked for 16 hr in 0.3% (v/v) ethyl methanesulfonate or for 4 hr in 10 mM diepoxybutane and then rinsed extensively with water. γ Mutagenesis was performed by soaking seeds in water for 3 hr and then exposing them to 60 krad in an irradiator (J.L. Shephard, Glendale, CA) containing ^{137}Cs . The mutagenized seed (M_1 generation) was sown and allowed to self-pollinate. M_2 progeny were collected and plated (on day 0) at a density of 300 to 400 seeds per 100-mm Petri plate containing 5 μM *N*-1-naphthylphthalamic acid (NPA), 5 μM 2-carboxyphenyl-3-phenylpropane-1,2-dione (CPD), or 0.1 μM methyl-2-chloro-9-hydroxyfluorene-9-carboxylate (CFM). To recover mutants with reduced sensitivity to growth inhibition by the compound, M_2 seedlings with roots longer than those of the wild-type controls were transferred on day 6 from

Table 3. Morphometric Analysis of the Wild Type and *tir3-1*

Measurement	Wild Type ^a	<i>tir3-1</i> ^a
Height of main inflorescence (cm)	46.5 ± 0.9	23.8 ± 0.7
Number of lateral branches on primary inflorescences	2.9 ± 0.1	3.4 ± 0.2
Number of siliques on primary inflorescences	33.2 ± 1.2	27.5 ± 1.6
Distance between siliques (mm)	11.3 ± 0.3	7.0 ± 0.3
Silique length (mm)	17.5 ± 0.2	9.8 ± 0.2
Pedical length (mm)	9.9 ± 0.2	3.8 ± 0.1
Number of secondary inflorescences	1.5 ± 0.2	3.8 ± 0.4
Number of lateral roots after 10 days	6.3 ± 0.4	0.0 ± 0.0
Root length after 8 days	42.2 ± 2.9	34.5 ± 3.0
Length of inflorescence epidermal cells (μm)	320 ± 8	200 ± 6
Length of root epidermal cells (μm)	259 ± 10	245 ± 8

^a ± SE.

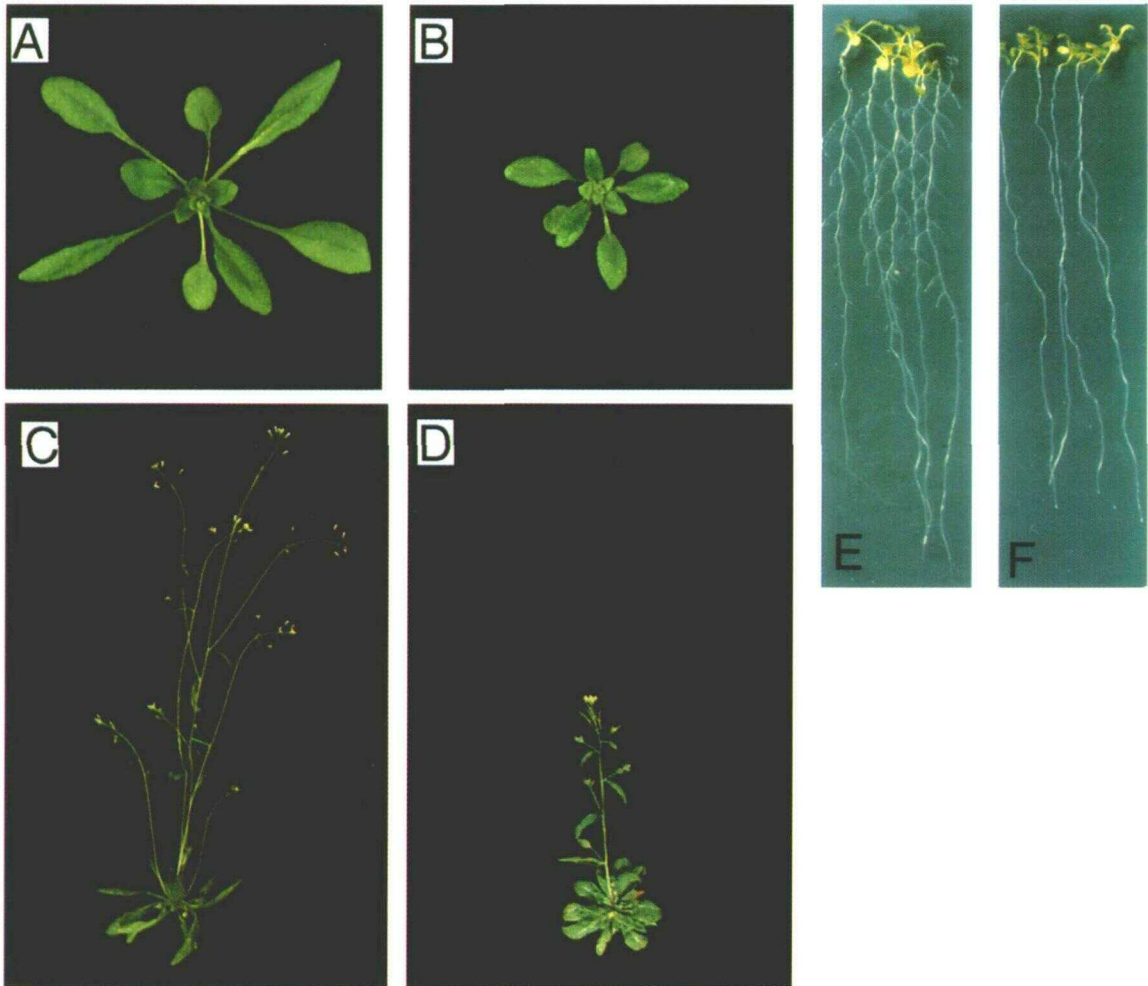


Figure 8. Morphology of Wild-Type and *tir3-1* Plants.

(A) and (B) Wild-type and *tir3-1* rosettes, respectively, photographed after 21 days of growth.

(C) and (D) Wild-type and *tir3-1* plants, respectively, photographed after 35 (C) and 41 (D) days of growth.

(E) and (F) Wild-type and *tir3-1* seedlings, respectively, grown on vertically oriented agar medium and photographed after 12 days.

the primary plates to secondary plates containing the same compound. After an additional week of growth, seedlings having roots that continued to grow more rapidly than did those of wild-type controls were transferred to potting mix.

Genetic Analyses

For genetic analyses, resistance to inhibition of root growth by a transport inhibitor was assayed by plating seed on a medium containing 5 μM CPD. Root growth was determined after 7 or 9 days. Resistance to 0.2 μM 2,4-D was assayed in a similar manner.

The *tir2*, *tir3*, *tir4*, *tir5*, *tir6*, and *tir7* mutants were all mapped using the *Arabidopsis* restriction fragment length polymorphism mapping set (ARMS) (Fabri and Schäffner, 1994). In each case, ~ 25 CPD-

resistant F_2 seedlings were scored for the 13 ARMS probes. Additional resolution was obtained for *tir3* by examining segregation of the simple sequence length polymorphism marker *nga172* in 25 F_2 plants of a *tir3-1* \times Landsberg *erecta* (*Ler*) cross (Bell and Ecker, 1994).

Morphometric Analysis

Seeds were sown at a density of 30 to 60 seeds per 13-cm pot. The pots were held at 4°C for 3 or 4 days and then transferred to a growth chamber set at 20°C. Illumination was continuous and consisted of $\sim 90 \mu\text{E m}^{-2} \text{sec}^{-1}$ of fluorescent light and $20 \mu\text{E m}^{-2} \text{sec}^{-1}$ of incandescent light. After germination, the seedlings were thinned to ~ 12 per pot and fertilized with the nutrient solution described above.

Measurements, as described in the text, were made after the plants had ceased flowering.

To determine the number of lateral roots, seeds were sown on nutrient medium in 82-mm Petri plates as described above. On day 3, seedlings were transferred to 150-mm Petri plates (containing the same medium), and the plates were returned to the incubator. On day 10, the number of lateral roots on each seedling was scored with the aid of a dissecting microscope.

To determine sensitivity to growth inhibitors, seeds were sown on inhibitor-free nutrient medium in 82-mm Petri plates, as described above. Three days after placing the plates in the incubator, seedlings were transferred to new plates containing the test compound. Five days later, roots were straightened, and growth over the previous five days was measured. Root growth was plotted as a percentage of growth on unsupplemented medium.

Fixation, Embedding, and Sectioning

Seedlings were grown vertically on nutrient medium for 7 days. Root tips were overlaid with 0.7% agar, and the root tip was cut 3 to 4 mm from the tip. Agar-embedded root tips were placed into freshly made cold 4% formaldehyde–1% glutaraldehyde in 0.05 M sodium phosphate, pH 7.2, with 0.02% Triton X-100. Root tips were fixed for 3 hr at 4°C, rinsed in cold sodium phosphate buffer, and postfixed overnight in 2% OsO₄ at room temperature. The root tips were then rinsed in sodium phosphate buffer, dehydrated through a graded ethanol series followed by acetone, and embedded in Spurr's resin. Thin sections (0.5 μm) were cut on a microtome (Sorvall, Newtown, CT) and then stained with 1% toluidine blue–1% borax. Stem tissue used for scanning electron microscopy was treated as described in Lincoln et al. (1990).

Auxin Transport Assays

Auxin transport assays were performed according to the method of Okada et al. (1991). Stem segments (2.5 cm) of primary inflorescence were incubated in a 1.5-mL Eppendorf centrifuge tube containing 30 μL of nutrient solution with 1 μM ¹⁴C–indole-3-acetic acid (IAA; 1.74 nCi/mL) with or without 15 μM NPA. The segments were incubated with their apical end in the solution for various times from 2 to 18 hr. After the incubation, a 5-mm section from the basal end of the segment was excised and added to 3 mL of liquid scintillation cocktail (Bio-Safe II; RPI, Mount Pleasant, IL). The samples were shaken at 100 rpm for at least 2 hr and left overnight at room temperature before scintillation counting in a scintillation counter (model LS 6500; Beckman Instruments). Individual experiments involved three stem segments for each time point. Stems incubated with the basal end in the solution transported low levels of ¹⁴C-IAA. Wild-type and *tir3* plants at the same developmental stage were chosen for the experiment. Because *tir3* bolts ~1 week later than do wild-type plants, the ages of the plants were 41 days for the wild type and 49 days for *tir3*. The plants were grown in 24 hr of light (105 μE m⁻² sec⁻¹), and the experiment was repeated three times with similar results.

Microsomal Membrane Preparation and ³H-NPA Binding Assays

For experiments on rosette leaves and mature roots, Arabidopsis seeds were sterilized and plated in dense lines on germination media

(1 × Murashige and Skoog salts [Gibco Laboratories, Grand Island, NY], 0.5 g/L Mes, 1% sucrose, 0.8% agar, and 0.05 mg/mL ampicillin, pH 5.8). Plates were placed at 4°C for 2 to 3 days in the dark to enhance germination. Plates were then placed upright under continuous light at 21°C in an incubator for ~3 weeks. Rosette microsomes were prepared according to the method of Dixon et al. (1996). ³H-NPA binding assays were performed in a 200-μL total volume of 20 mM sodium citrate, pH 5.3, 1.0 mM MgCl₂, and 0.25 M sucrose (NBB) with microsomes at a final concentration of 0.2 mg/mL. Microsomes were incubated with ³H-NPA concentrations ranging from 2 to 15 nM in the presence or absence of 10 μM cold NPA, as described by Muday et al. (1993). The addition of unlabeled NPA allowed us to measure the background or nonspecific binding. Samples were incubated at 4°C with shaking for 1 hr. After incubation, samples were filtered over 0.3% polyethylenimine-treated glass fiber (GFB) filters (Whatman) and washed with 5 mL of NBB, as described by Dixon et al. (1996).

To characterize NPA binding in seedlings, Arabidopsis seeds were germinated aseptically in a liquid medium composed of half-strength Murashige and Skoog salts supplemented with 2% sucrose. Seedlings were harvested after 3 days of growth in the dark under mild agitation at room temperature. Total microsome fraction was prepared as described above. NPA binding assays were conducted using 40 μg of protein per sample. Samples were incubated for 2 hr at 4°C with 10 nM ³H-NPA in a volume of 200 μL of NBB (Muday et al., 1993). Nonspecific binding was determined in the presence of 10 μM cold NPA. Bound ³H-NPA was separated from free ³H-NPA by filtering over GFB filters and presoaked in 0.1% polyethylenimine (Bruns et al., 1983). The filters were washed with 5 mL of cold PM buffer and counted in 4 mL of cocktail mix (Ready Protein; Beckman Instruments).

ACKNOWLEDGMENTS

We thank Dr. F. Rudolf Turner for his help with sectioning and scanning electron microscopy and Dr. Gerard Katekar for his generous gift of CPD. We also thank members of the Estelle laboratory and the Indiana University Arabidopsis group for stimulating discussion throughout the course of this work. This research was supported in part by grants from the National Science Foundation (No. PCM8212660 for scanning electron microscopy facility, postdoctoral fellowship No. MCB-9008316 to L.H., Eli Lilly/Indiana Institute for Molecular Biology predoctoral fellowship to M.R., No. IBN9318250 to G.M., and No. IBN-9307134 to M.E.), National Aeronautics and Space Administration (No. NAGW-4052 to G.M.), and National Institutes of Health (No. PHS-GM43644 to M.E.).

Received January 7, 1997; accepted March 17, 1997.

REFERENCES

- Bell, C.J., and Ecker, J.R. (1994). Assignment of 30 microsatellite loci to the linkage map of *Arabidopsis*. *Genomics* **19**, 137–144.
- Bennett, M.J., Marchant, A., Green, H.G., May, S.T., Ward, S.P., Millner, P.A., Walker, A.R., Schulz, B., and Feldmann, K.A. (1996). *Arabidopsis AUX1* gene: A permease-like regulator of root gravitropism. *Science* **273**, 948–950.

- Bennett, S.R.M., Alvarez, J., Bossinger G., and Smyth, D.** (1995). Morphogenesis in *pinoid* mutants of *Arabidopsis thaliana*. *Plant J.* **8**, 505–520.
- Berlith, T., and Jurgens, G.** (1993). The role of the *monopteros* gene in organising the basal body region of the *Arabidopsis* embryo. *Development* **118**, 575–587.
- Bernasconi, P., Patel, B.C., Reagan, J.D., and Subramanian, M.V.** (1996). The *N*-1-naphthylphthalamic acid-binding protein is an integral membrane protein. *Plant Physiol.* **111**, 427–432.
- Bruns, R.F., Lawson-Wendling, K., and Pugsley, T.A.** (1983). A rapid filtration assay for soluble receptors using polyethylenimine-treated filters. *Anal. Biochem.* **132**, 74–81.
- Carland, F.M., and McHale, N.A.** (1996). *LOP1*: A gene involved in auxin transport and vascular patterning in *Arabidopsis*. *Development* **122**, 1811–1819.
- Celenza, J.L., Grisafi, P.L., and Fink, G.R.** (1995). A pathway for lateral root formation in *Arabidopsis thaliana*. *Genes Dev.* **9**, 2131–2142.
- Cox, D.N., and Muday, G.K.** (1994). NPA binding activity is peripheral to the plasma membrane and is associated with the cytoskeleton. *Plant Cell* **6**, 1941–1953.
- Davies, P.J., and Rubery, P.H.** (1978). Components of auxin transport in stem segments of *Pisum sativum*. *Planta* **142**, 211–219.
- Delbarre, A., Muller, P., Imhoff, V., and Guern, J.** (1996). Comparison of mechanisms controlling uptake and accumulation of 2,4-dichlorophenoxyacetic acid, naphthalene-1-acetic acid, and indole-3-acetic acid in suspension-culture tobacco cells. *Planta* **198**, 532–541.
- Dixon, M.W., Jacobson, J.A., Cady, C.T., and Muday, G.K.** (1996). Cytoplasmic orientation of the naphthylphthalamic acid-binding protein in zucchini plasma membrane vesicles. *Plant Physiol.* **112**, 421–432.
- Dolan, L., Janmaat, K., Willemsen, V., Linstead, P., Poethig, S., Roberts, K., and Scheres, B.** (1993). Cellular organization of the *Arabidopsis thaliana* root. *Development* **119**, 71–84.
- Evans, M.L.** (1991). Gravitropism: Interaction of sensitivity, modulation, and effector redistribution. *Plant Physiol.* **95**, 1–5.
- Fabri, C.O., and Schäffner, A.R.** (1994). An *Arabidopsis thaliana* RFLP mapping set to localize mutations to chromosomal regions. *Plant J.* **5**, 149–156.
- Garbers, C., DeLong, A., Deruere, J., Bernasconi, P., and Soll, D.** (1996). A mutation in protein phosphatase 2A regulatory subunit A affects auxin transport in *Arabidopsis*. *EMBO J.* **15**, 2115–2124.
- Hobbie, L., and Estelle, M.** (1995). The *axr4* auxin-resistant mutants of *Arabidopsis thaliana* define a gene important for root gravitropism and lateral root initiation. *Plant J.* **7**, 211–220.
- Jacobs, M., and Rubery, P.H.** (1988). Naturally occurring auxin transport regulators. *Science* **241**, 346–349.
- Katekar, G.F., and Geissler, A.E.** (1977). Auxin transport inhibitors. III. Chemical requirements of a class of auxin transport inhibitors. *Plant Physiol.* **60**, 826–829.
- Kerk, N., and Feldman, L.** (1994). The quiescent center in roots of maize: Initiation, maintenance and role in organization of the root apical meristem. *Protoplasma* **183**, 100–106.
- Kerk, N., and Feldman, L.J.** (1995). A biochemical model for initiation and maintenance of the quiescent center: Implications for organization of root meristems. *Development* **121**, 2825–2833.
- Koomneef, M., and Stam, P.** (1992). Genetic analysis. In *Methods in Arabidopsis Research*, C. Koncz, N.-H. Chua, and J. Schell, eds (Singapore: World Scientific), pp. 83–99.
- Lincoln, C., Britton, J.H., and Estelle, M.** (1990). Growth and development of the *axr1* mutants of *Arabidopsis*. *Plant Cell* **2**, 1071–1080.
- Lister, C., and Dean, C.** (1993). Recombinant inbred lines for mapping RFLP and phenotypic markers in *Arabidopsis thaliana*. *Plant J.* **4**, 745–750.
- Lomax, T.L., Muday, G.K., and Rubery, P.H.** (1995). Auxin transport. In *Plant Hormones: Physiology, Biochemistry, and Molecular Biology*, P.J. Davies, ed (Dordrecht, The Netherlands: Kluwer Academic Publishers), pp. 509–530.
- Meuwly, P., and Pilet, P.-E.** (1991). Local treatment with indole-3-acetic acid influences differential growth responses in *Zea mays* L. roots. *Planta* **185**, 58–64.
- Morris, D.A., and Thomas, A.G.** (1978). A microautoradiographic study of auxin transport in the stem of intact pea seedlings (*Pisum sativum* L.). *J. Exp. Bot.* **29**, 147–157.
- Morris, D.A., Rubery, P.H., Jarman, J., and Sabater, M.** (1991). Effects of inhibitors of protein synthesis on transmembrane auxin transport in *Cucurbita pep.* *J. Exp. Bot.* **42**, 773–783.
- Muday, G.K., and Haworth, P.** (1994). Tomato root growth, gravitropism and lateral development: Correlations with auxin transport. *Plant Physiol. Biochem.* **32**, 193–203.
- Muday, G.K., Brunn, S.A., Haworth, P., and Subramanian, M.** (1993). Evidence for a single naphthylphthalamic acid binding site on the zucchini plasma membrane. *Plant Physiol.* **103**, 449–456.
- Muday, G.K., Lomax, T.L., and Rayle, D.L.** (1995). Characterization of the growth and auxin physiology of roots of the tomato mutant, *diageotropica*. *Planta* **195**, 548–553.
- Okada, K., Ueda, J., Komaki, M.K., Bell, C.J., and Shimura, Y.** (1991). Requirement of the auxin polar transport system in early stages of *Arabidopsis* floral bud formation. *Plant Cell* **3**, 677–684.
- Przemeczek, G.K.H., Mattsson, J., Hardtke, C.S., Sung, Z.R., and Berleth, T.** (1996). Studies on the role of the *Arabidopsis* gene *MONOPTEROS* in vascular development and plant axialization. *Planta* **200**, 229–237.
- Reed, R.C., and Muday, G.K.** (1996). *Arabidopsis* lateral root development requires auxin from the shoot. *Plant Physiol.* **111** (suppl.), 134 (abstr.).
- Suttle, J.C.** (1991). Biochemical bases for the loss of basipetal IAA transport with advancing physiological age in etiolated *Helianthus* hypocotyls. *Plant Physiol.* **96**, 875–880.
- Tamas, I.A.** (1995). Hormonal regulation of apical dominance. In *Plant Hormones: Physiology, Biochemistry, and Molecular Biology*, P.J. Davies, ed (Dordrecht, The Netherlands: Kluwer Academic Publishers), pp. 572–597.
- Tsurumi, S., and Ohwaki, Y.** (1978). Transport of ¹⁴C-labeled indoleacetic acid in *Vicia* root segments. *Plant Cell Physiol.* **19**, 1195–1206.
- Wightman, F., and Thimann, K.V.** (1980). Hormonal factors controlling the initiation and development of lateral roots. *Physiol. Plant.* **49**, 13–20.